Quantification of [^{123}I]FP-CIT SPECT brain images: an accurate technique for measurement of the specific binding ratio

Livia Tossici-Bolt[1], Sandra M. A. Hoffmann[1], Paul M. Kemp[2], Rajnikant L. Mehta[3], John S. Fleming[1]

[1] Department of Medical Physics and Bioengineering, Southampton University Hospital NHS Trust, Tremona Road, Southampton, SO16 6YD, UK
[2] Department of Nuclear Medicine, Southampton University Hospitals NHS Trust, Tremona Road, Southampton, SO16 6YD, UK
[3] Public Health Sciences and Medical Statistics/Research and Development Support Unit, School of Medicine, University of Southampton, Southampton, UK

Received: 22 June 2005 / Accepted: 14 April 2006 / Published online: 21 July 2006

Abstract. *Purpose:* A technique is described for accurate quantification of the specific binding ratio (SBR) in [^{123}I] FP-CIT SPECT brain images.
Methods: Using a region of interest (ROI) approach, the SBR is derived from a measure of total striatal counts that takes into account the partial volume effect. Operator intervention is limited to the placement of the striatal ROIs, a task facilitated by the use of geometrical template regions. The definition of the image for the analysis is automated and includes transaxial slices within a "slab" approximately 44 mm thick centred on the highest striatal signal. The reference region is automatically defined from the non-specific uptake in the whole brain enclosed in the slab, with exclusion of the striatal region. A retrospective study consisting of 25 normal and 30 abnormal scans—classified by the clinical diagnosis reached with the scan support—was carried out to assess intra- and inter-operator variability of the technique and its clinical usefulness. Three operators repeated the quantification twice and the variability was measured by the coefficient of variation (COV).
Results: The COVs for intra- and inter-operator variability were 3% and 4% respectively. A cutoff ~4.5 was identified that separated normal and abnormal groups with a sensitivity, specificity and diagnostic concordance of 97%, 92% and 95% respectively.
Conclusion: The proposed technique provides a reproducible and sensitive index. It is hoped that its independence from the partial volume effect will improve consistency in quantitative measurements between centres with different imaging devices and analysis software.

Livia Tossici-Bolt (✉)
Department of Medical Physics and Bioengineering,
Southampton University Hospital NHS Trust,
Tremona Road,
Southampton, SO16 6YD, UK
e-mail: livia.bolt@suht.swest.nhs.uk
Tel.: +44-23-80795055

Keywords: Brain SPECT – Dopamine transporters – Quantification – Specific binding – Operator reproducibility

Eur J Nucl Med Mol Imaging (2006) 33:1491–1499
DOI 10.1007/s00259-006-0155-x

Introduction

[^{123}I]FP-CIT is a useful tracer in brain single-photon emission computed tomography (SPECT) imaging for assessing the availability of dopamine transporters (DATs) in the corpus striatum, and thus the functionality of the nigrostriatal dopaminergic neurons. It is proving an effective tool in neurology, in helping to differentiate Parkinson's disease (PD) and parkinsonian syndromes (PS: progressive supranuclear palsy and multiple system atrophy) from essential tremor (ET) [1–3], and in psychiatry, in assisting in the differential diagnosis of dementia with Lewy bodies (DLB) from Alzheimer's disease (AD) [4–6]. Visual interpretation of the images gives high diagnostic accuracy. This is because the reduction of signal in parkinsonism is large, and distinctly pronounced in subregions of the striatum, involving mainly the putaminal tail in the early stages of the disease [7–10] and then advancing towards the putaminal body and the caudate nucleus as the disease progresses, although early abnormal decrease in the caudate has been reported in some cases [11]. In patients with DLB, there is some evidence that the reduction of signal is of similar magnitude but more widespread throughout the striatum, with a smaller difference between uptakes of caudate nucleus and putamen [5, 6]. Quantification, however, offers a non-subjective adjunct to visual interpretation, and can be particularly valuable to assess images with subtle reductions, rather than disappearance of putamen activity. Furthermore, quantification is a sensitive aid in early detection of the disease in monitoring its progression [12].

Absolute quantification of dopamine transporters requires full kinetic modelling, with invasive arterial blood sampling and dynamic SPECT scanning, which is impractical in a clinical setting. A number of kinetic studies of various radiopharmaceuticals for DAT imaging have also investigated the feasibility of simplified scan protocols and of semiquantitative methods under conditions of equilibrium binding [10, 13–15]. A good correlation has been demonstrated between a semiquantitative index of the specific DAT binding—referred to as the "specific binding ratio" (SBR)— with the accurate kinetic parameter. This has led to the conclusion that such an empirical index is directly proportional to the density of DATs in equilibrium. This equilibrium condition is approximately satisfied between 3 and 6 h after injection for [^{123}I]FP-CIT [14], although there is a small but not negligible difference in the washout of specific and non-specific binding [14] that makes the issue of the study timing important in quantification.

Although the SBR definition in literature is based on a common philosophy—the measurement of count concentrations in the striatal region and in a reference region devoid of DATs—its implementation varies considerably. Differences are found in the choice of the reference region and in its size, and in the shape and size of the striatal regions. The size of these volumes of interest, in particular, has a direct impact on the measurement of count concentration. This is mainly a consequence of the poor spatial resolution of SPECT imaging, which causes counts to be blurred out of the physical volume of the structure (partial volume effect), and therefore makes it difficult to evaluate count concentrations with accuracy.

This study attempts to define a method for accurately measuring the specific to non-specific ratio. It is essentially based on a measure of the total counts in the striatum, rather than count concentration, which allows account to be taken of the partial volume effect. Geometrical volumes of interest (VOIs) are used for the striatum, large enough to ensure the inclusion of all the partial volume counts detected outside the physical volume of the structures. The added advantage of using geometrical shapes is a reduced operator-introduced variability in their positioning. The definition of the reference region has been fully automated.

The retrieval of partial volume counts, combined with the automation of the definitions of the image for the analysis and of the reference region, contributes to the robustness to the technique. Intra- and inter-observer variability have been evaluated and compared to a manual technique [16, 17] that similarly measures total striatal counts.

Materials and methods

The quantitative technique was applied to a set of 55 scans randomly chosen from the database of patients referred to our department for a [^{123}I]FP-CIT SPECT scan (DeTSCAN, GE Healthcare) with symptoms suggestive of PD, PS or ET. The patients were referred by consultants with a special interest in movement disorders upon presentation of their symptoms, and were therefore regarded as potentially having very early disease. The group consisted of 25 "normal" subjects and 30 "abnormal" subjects, the classification into these two categories being based on the clinical diagnosis reached by the referring consultants taking into account the report of the SPECT investigation and subsequent patient follow-up over the following years. "Normal" therefore means exclusion of PD or PS in the final diagnosis. The normal group consisted of nine (36%) women and 16 (64%) men, and the abnormal group, of 14 (47%) women and 16 (53%) men. The normal group was age matched (mean±SD 69.6±9.6 years, range 49–85 years) with the abnormal group (mean±SD 67.7±9.4 years, range 46–86 years).

SPECT imaging

All medications which may affect DAT binding were curtailed prior to scanning in accordance with the DeTSCAN manufacturer's instructions. Each patient received thyroid blocking 15 min prior to intravenous injection of a bolus dose of 185 MBq of [^{123}I]FP-CIT. The mean (±SD) imaging times post injection were 3 h 23 min (±32 min) and 3 h 26 min (±24 min) for the normal and abnormal groups respectively. Images were acquired using a two-head GE DST-XL gamma camera equipped with low-energy high-resolution collimators. One hundred and twenty-eight projection images were obtained over 360° by rotating each head 180° following an elliptical contour, where the radius of rotation was minimised for each subject. The matrix size was 128×128, and the magnification factor of 1.33 gave a pixel size of 3.38 mm. Counts were acquired within a 20% symmetrical energy window centred around 159 keV.

Reconstruction was performed on a Link workstation using MAPS-10000 software. Raw projections were filtered prior to reconstruction with a Butterworth filter, cutoff 0.20 cycles/pixel and order 10. Transaxial slices covering the whole brain were reconstructed using filtered back projection with a ramp. Attenuation correction was applied during reconstruction using the first-order Chang method based on a uniform elliptical region of interest manually fitted to the maximum cross-section of the head and using a linear attenuation coefficient of 0.113 cm^{-1}. Correction for scatter and septal penetration was not performed. The transaxial slices, one pixel thick, were manually corrected for possible transverse and coronal inclinations and reoriented parallel to standardised orientation of the orbito-meatal (OM) plane.

The reconstructed images were then submitted to quantification. The quantification algorithm, written using MAPS-10000 software, is described in the following sections and summarised in the flowchart in Fig. 1.

Definition of the specific binding ratio

The [^{123}I]FP-CIT image can be regarded as the contribution of (a) the "specific uptake" of the tracer in the striata and (b) the "non-specific" uptake (non-specifically bound and free tracer) in the whole brain cortex, striata included. The specific binding ratio SBR is defined as the ratio between the concentrations of the specific to the non-specific radioactivity bound to the striatum. The non-specific uptake is estimated from a region of the brain devoid of DATs, taken as the reference region. The assumption is made of equivalent non-specific uptake in the striatal and reference regions.

The SBR can therefore be defined as:

$$\mathrm{SBR} = c_s/c_r \quad (1)$$

where c_s is the count concentration in the striatum due to the specific binding only and c_r is the count concentration in a reference region due to the non-specific binding.

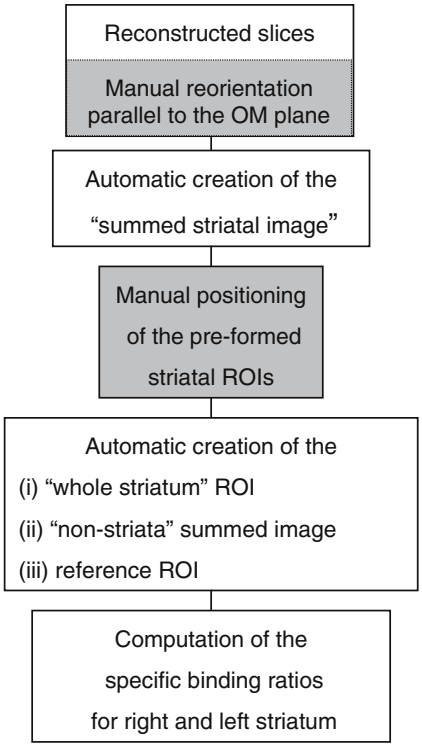

Fig. 1. Flow diagram of the quantification algorithm. The input data are the reconstructed transverse images, oriented in the OM plane. The semi-automated algorithm includes four main steps: the creation of the "summed" image for the analysis (automated), the placement of the striatal ROIs (manual), the creation of the reference ROI (automated) and the calculation of the SBRs for right and left striatum. Manual intervention is highlighted in *grey*

The count concentration c_r is simply the mean counts per pixel in the reference VOI. The specific count concentration c_s is unknown, but can be accurately estimated from the total counts in the striatal VOI, the quantity actually measured, provided that the striatal VOI is big enough to include *all* the counts originating from the tracer uptake in the corpus striatum. The algorithm uses striatal VOIs of geometrical shape (rather than anatomical) and generous size, which sample the entire striatal structure as well as the adjacent space containing partial volume counts. The use of an anatomical VOI that perfectly fits the striatum would, in fact, underestimate the striatal counts because of the partial volume effect. The large VOI adopted in this technique, however, will also include "background" counts, which need to be subtracted in order to assess correctly c_s. This subtraction can be easily performed according to the following procedure.

Let Ct_{VOI} be the total counts in the striatal VOI, which can be expressed as the sum of the counts originating from the specific activity in the striatum, Ct_s, and those originating from the non-specific activity throughout the whole striatal VOI, Ct_{ns}:

$$Ct_{VOI} = Ct_s + Ct_{ns} \quad (2)$$

Assuming that the non-specific uptake is similar throughout the cortex, Ct_{ns} can be estimated from the counts concentration in the reference region c_r, by simply multiplying c_r by the volume of the striatal VOI, V_{VOI}:

$$Ct_{ns} = c_r \times V_{VOI} \quad (3)$$

The striatal counts due to the specific uptake of the tracer are therefore found by substitution of Eq. 3 in Eq. 2:

$$Ct_s = Ct_{VOI} - c_r \times V_{VOI} \quad (4)$$

It is possible to define an index of the specific uptake as:

$$SUSI = Ct_s/c_r = Ct_{VOI}/c_r - V_{VOI} \quad (5)$$

This is refereed to as the Specific Uptake Size Index (SUSI) and has units of volume [18]. Provided that the VOI is sufficiently large to include all counts associated with striatal activity, this index has been demonstrated to be independent from the size of the VOI and from the resolution of the system [18].

If the volume of the striatum (V_s) is known, then the specific count concentration in the striatum c_s can be calculated:

$$c_s = Ct_s/V_s \quad (6)$$

By substituting Eqs. 4 and 6 in Eq. 1, the SBR can be expressed in terms of the measurable quantities Ct_{VOI} and c_r:

$$SBR = SUSI/V_s = (1/V_s)\{Ct_{VOI}/c_r - V_{VOI}\} \quad (7)$$

As the volume of the striatum V_s is generally unknown for each subject (unless a structural MRI or CT scan is available), a standard value of V_s=11.2 ml has been assumed in the algorithm. This value coincides with the volume of the striatal vessels of the brain phantom from Radiology Support Devices (RSD, PI Medical Diagnosis Equipment B.V., The Netherlands), and it is representative of the normal range reported in literature [19, 20]. This assumption is not critical, as V_s appears only as a scaling factor in Eq. 7: essentially the SBR is a measure of the total uptake in the striata.

In the following, the three main steps carried out by the semi-automated algorithm for the calculation of the SBRs are described: the automatic definition of the image for the analysis, the manual placement of the template VOIs on the striatum and the automatic definition of the reference region.

Automatic creation of the "summed striatum image"

The 3D problem of quantifying the tracer uptake in a 3D structure can be effectively reduced to a 2D problem by creating a "summed striatum image" of all the transaxial slices covering the striatum. The choice of the range of slices to be included, however, is a process open to subjectivity, mainly because the blurring of partial volume counts makes it difficult for the operator to definitely identify the upper and lower slices containing striatal uptake. This process has therefore been automated. The algorithm identifies the slice containing the hottest striatal voxel and considers it to be the central slice of the summed image. A fixed number of slices on either side are then added together to form a "slab" approximately 44 mm thick, which comfortably includes all striatal counts. In the case of our pixel size of 3.38 mm, the slab consists of 13 slices. The algorithm offers the operator the possibility to check and re-centre the slab, should the automated centring be unsatisfactory. The summed striatum image is then obtained by summing all the slices in the slab.

The striatal VOIs: right, left and "whole"

The use of the summed image of the striatum enables the analysis to be carried out with 2D regions (ROIs) rather than volumes of interest. The algorithm uses two pre-formed striatal ROIs, which are manually positioned by the operator over the right and left striatum in the summed image. The placement of these ROIs is the only source of operator variability in the technique, which can be minimised by the use of template ROIs of standard shape and dimensions. The generous dimensions of approximately 61 mm×48 mm (Fig. 2) ensure the inclusion of all striatal counts, including those blurred outside the actual structure because of the partial volume effect. Rotations are not allowed—in fact they are made redundant by the large dimensions of the ROIs—but only shifting in the anterior–posterior and lateral directions.

The correct placement of the regions must only rely on the uptake in the caudate nucleus, as in abnormal studies the putamen tail is partially visible or not visible at all. The anterior border of each ROI must be aligned with the anterior border of the corresponding caudate nucleus, leaving a reasonable margin (about 2 pixels) for partial volume counts. The lateral alignment relies mainly on the medial borders of the ROIs and of the striata; the medial borders of the two ROIs may coincide, lying along the mid-lane of the striata, but not overlap. Examples of striatal ROI positioning are shown in Fig. 3 for a normal and an abnormal scan.

Once the operator is satisfied with the position of these two ROIs, the algorithm automatically creates a third region, the "whole striatum" ROI, the rectangular box shown in Fig. 4a. This region is defined as the rectangle that encompasses both right and left striatal ROIs and any space between them. The sole purpose of the whole striatum ROI is to assist the automated definition of the reference region, as described in the following.

The reference VOI

The reference region provides an estimate of the non-specific uptake concentration.

Rather than choosing a particular region devoid of DATs, the approach has been adopted to incorporate the whole brain—other than the striatal region—included in the summed image. The main reason for this choice is that the non-specific uptake within the striatal ROI and in the various subregions of the grey matter shows a variable degree of heterogeneity between subjects. Furthermore, the partial volume effect causes blurring of counts from the grey matter into the ventricular space, often to such an extent that the ventricles

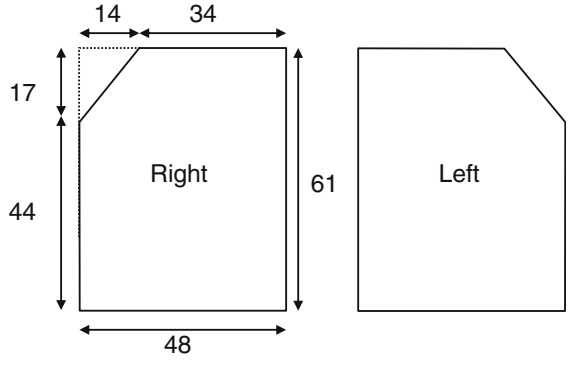

Fig. 2. Schematic diagram showing the dimensions of the striatal ROIs in mm

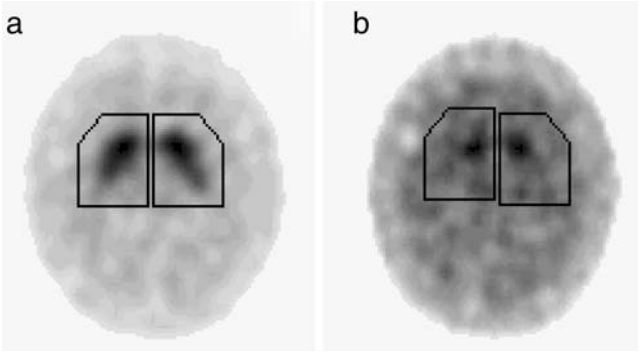

Fig. 3. Manual placement of the striatal ROIs: examples in a normal (**a**) and an abnormal (**b**) scan

are practically indistinguishable, sometimes making it difficult to use confidently occipital or frontal cortex regions. The proposed use of the overall non-specific cortex should reduce variability as well as improve counting statistics.

The definition of this ROI has been fully automated; examples illustrative of the steps involved are shown in Fig. 4. The procedure uses a threshold technique based on the maximum pixel counts value of the "non-specific" uptake, M_{ns}. In order to extract M_{ns} from the summed image, the whole striatum ROI is first "masked" by setting its counts to zero. The resulting image, which contains non-striatal uptake only, is then smoothed three times and M_{ns} derived (Fig. 4a). Smoothing is desirable as it reduces statistical fluctuation, thus ensuring that the maximum of the non-specific uptake does not represent a statistical extreme value.

In order to be able to define an iso-contour based on M_{ns}, any pixel count within the "whole striata" ROI that is above M_{ns} needs to be set to the value M_{ns} (Fig. 4b). The resulting image is then heavily smoothed (20 times)—merely to ensure that the contour will be smooth in outline—and the iso-contour region at a threshold of 50% of M_{ns} created (Fig. 4c). Finally the reference ROI is obtained by bringing this contour inward by 6 pixels (~20 mm) in order to exclude the periphery of the head, where partial volume is significant (Fig. 4d). The mean counts in this region are assumed to represent the non-specific uptake within the striatal ROIs.

Statistical analysis

In a first study, we tested the reproducibility of the quantification technique in its own right, or "intrinsic" reproducibility, which excludes the operator-dependent step of the OM reorientation (Fig. 1). One operator reconstructed and aligned the 55 DaTSCANs in the OM plane, and then the images were given to four operators for the analysis. One of them was entirely inexperienced and was first introduced to the technique using a series of test images. The three experienced operators then progressed into a second study aiming to assess the reproducibility of the quantification technique when the variation associated with the OM reorientation was included in the process. They were asked first to perform the OM alignment and then to proceed with the quantification. The two reproducibility studies were undertaken 6 months apart; in both one operator repeated the quantification twice about 1 month apart.

Intra- and inter-operator variability were assessed by the coefficient of variation (COV) [21]:

$$\mathrm{COV}(\%) = 100 \times \mathrm{SD}/\mathrm{SBR}_{\mathrm{m}} \qquad (8)$$

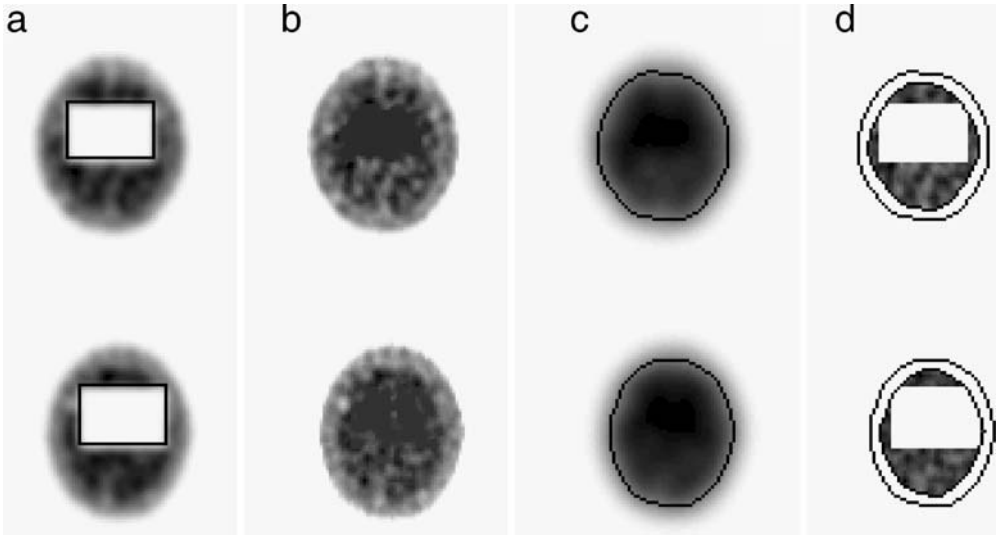

Fig. 4. Automatic definition of the reference ROI: the examples correspond to the normal (*above*) and abnormal (*below*) scans used in Fig. (3). The "non-specific" maximum M_{ns} is extracted from the smoothed summed image in which all pixels within the striatal ROI have been set to zero (**a**). In the original summed image, all counts within the striatal ROI above M_{ns} are set to M_{ns} (**b**). The resulting image is smoothed 20 times and a 50% iso-contour is defined based on M_{ns} (**c**). The reference ROI is finally obtained by "erosion" of the iso-contour by ~20 mm inwards, to exclude the edge of the cortex (**d**)

where SBR_m and SD are the pooled mean and standard deviation of the SBRs measurement on the N subjects (i=1,...,N=55), carried out either by the different operators (j=1,...,Op, where Op is 3 or 4) or repeated twice by the same operator (Op=2):

$$SBR_m = \frac{\sum_{i=1}^{N}\sum_{j=1}^{Op} SBR_{ij}}{N \times Op} \qquad (9)$$

$$SD = \sqrt{\frac{(M_1 - 1)SD_1^2 + ... + (M_N - 1)SD_N^2}{(M_1 - 1) + ... + (M_N - 1)}}$$

with M_i the number of operators responsible for the analysis of the ith subject (in general M_i may differ from one subject to another). In this study, each subject has been analysed by all operators and therefore M_i=Op for all subjects. The expression for the pooled standard deviation becomes:

$$SD = \sqrt{\frac{1}{N}\sum_{i=1}^{N} SD_i^2} = \sqrt{\frac{\sum_{i=1}^{N}\sum_{j=1}^{Op}(SBR_{ij} - SBR_{mi})^2}{N \times (Op - 1)}} \qquad (10)$$

The means of the measurements carried out by the operators were tested for the presence of any systematic difference using the paired t test (for intra-operator difference) and analysis of variance (ANOVA) (for inter-operator difference). Results were presented as (mean± standard deviation: mean±σ). The means in the normal and abnormal groups were tested for significant difference using the independent t test assuming equal variance.

The reliability of the technique was assessed using the intraclass correlation coefficient (ICC): [21]:

$$ICC = (MSB - MSW)/(MSB + (k - 1) \times MSW) \qquad (11)$$

where MSB and MSW are the mean sum of squares between and within subject measurements, and k is the number of within-subject measurements (k=4). ICC ranges from 0 (no reliability) to 1 (total reliability). Variances between and within subjects were obtained from the ANOVA analysis.

Finally, intra- and inter-observer (intrinsic) variability were compared with those of an existing method of quantification [16] which also uses rectangular (rather than anatomical) ROIs but which demands a higher degree of operator intervention. Essentially, this technique requires the operator to define the thickness of the striatal slab, ensuring that it extends beyond the visually identified striatum by one slice at both extremities. The operator is also required to position large rectangular ROIs over striata and posterior (occipital) regions. All ROIs are identical in size; therefore the specific striatal counts Ct_s are obtained by subtracting the total counts in the reference VOI (Ct_r) from the total counts in a striatal VOI (Ct_t). This technique defines the specific binding index as:

$$Ct_s/Ct_r = (Ct_t - Ct_r)/Ct_r \qquad (12)$$

which is proportional to the absolute SBR of Eq. 1. Two experienced operators applied this method to the same set of OM reoriented images used in the "intrinsic" reproducibility study, one operator twice. Intra and inter COVs and ICC were derived and compared with those of the proposed technique. This allowed the impact on reproducibility of subjective factors other than striatal ROI placement to be assessed. COVs were compared with the F test.

Results

The intra- and inter-observer coefficients of variation measured from the first reproducibility study were COV_{intra}=2% and COV_{inter}=2.5%. This study tested the "intrinsic" variability of the technique, solely associated with the subjective placement of the striatal ROIs. They were compared with the corresponding coefficients obtained from the manual technique of Eq. 12, which were found to be significantly higher, at 6% and 11% respectively (p<0.001). As expected, additional subjective factors, such as the choice of the thickness of the summed image and the placement of the reference region, have a significant impact on reproducibility.

The results of the second reproducibility study, which included the variability associated with the manual reorientation to the OM plane in the quantification process, are shown in the Bland-Altman plots [22] in Fig. 5. The plots compare the measurements of the SBRs of right and left sides of the striatum repeated by the same operator (Fig. 5a)

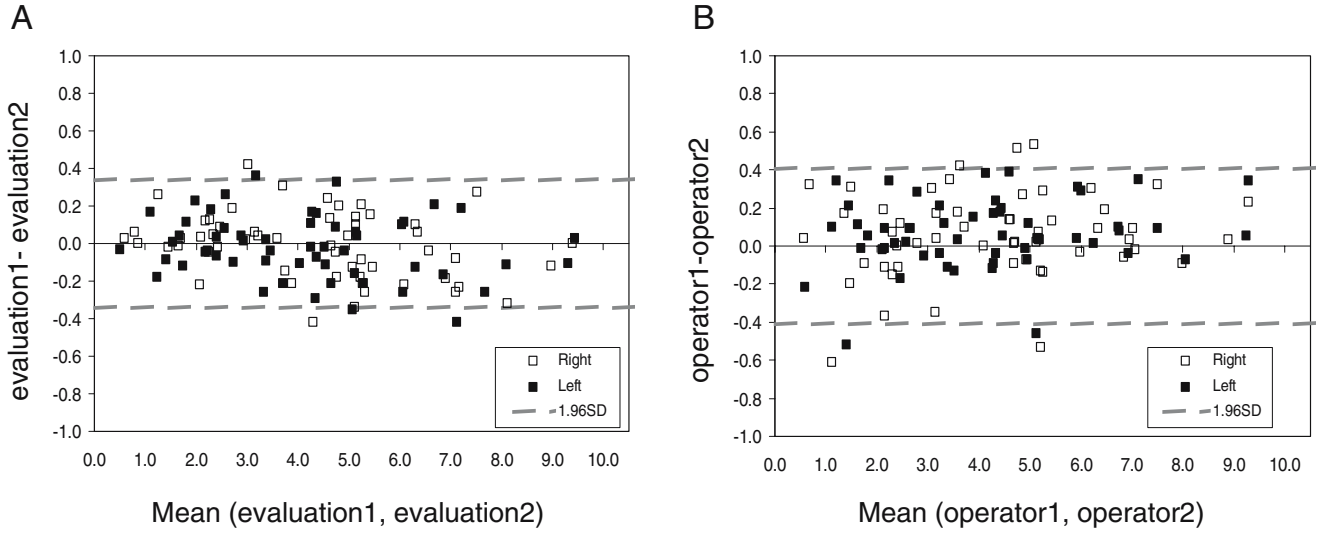

Fig. 5. Variability of SBR measurements: intra-operator (**a**) and inter-operator (**b**) measurements. *Open and filled squares* refer to the right and left striatum SBRs respectively. Also shown are the ±1.96σ limits of the observed differences

and obtained by two (of the three) different operators (Fig. 5b). Plots similar to Fig. 5b are obtained from the combination of any two of the three operators who took part in the study. The data are tightly grouped around the identity line (difference=0); the differences are distributed with a mean (±σ) of 0.02 (±0.17) for the intra-operator and 0.06 (±0.20) for the inter-operator data. The ±1.96σ limits are also shown with the plots. The COVs for intra- and inter-operator variability were COV_{intra}=3% and COV_{inter}=4%. They are marginally higher than the "intrinsic" coefficients, but the *F* test found that the difference reached statistical significance only for COV_{intra} (p~0.05).

In clinical practice it is the lowest SBR between right and left striatum that is relevant, since the presence of abnormal uptake at least on one side of the striatum suffices to hold the study as quantitatively abnormal. The following statistical analysis is therefore concerned with the side of the striatum with lower uptake. The mean (±σ) intervals of the SBR obtained from the repeated measurements by the first operator were 5.83 (±1.54) and 5.87 (±1.58) for the normal group and 2.60 (±1.16) and 2.58 (±1.20) for the abnormal group. Similarly, the intervals measured by the second operator for the two groups were 5.74 (±1.53) and 2.55 (±1.14), and those measured by the third operator were 5.80 (±1.48) and 2.51 (±1.23). The paired *t* test applied to the repeated measurements by the same operator found no evidence of statistically significant difference (p=0.315); similarly, the ANOVA analysis did not find any significant difference between the inter-operator measurements (p=0.974). The intraclass correlation coefficient (Eq. 11) demonstrated excellent reliability of the technique: ICC was 0.99 for both reproducibility studies. The ICC for the manual technique was of similar magnitude (0.94).

The measurements of the SBR ratios obtained by operator 1 are plotted in Fig. 6 for the two groups diagnosed as normal and abnormal. Again, only the lowest SBR ratios between right and left striatum are shown. Overall, the two groups show a separation, although there is some overlap around the value of SBR ~4.5. The level of overlap seems consistent with previous studies [11, 12]. The mean SBR in the abnormal group, 2.53 (±1.15), is significantly lower than that in the normal group, 5.83 (±1.53) (p<0.001).

By optimising the diagnostic concordance, a cutoff ~4.5 was identified for the SBR (shown in Fig. 6), which separates normality (above) from abnormality (below) with a sensitivity and specificity of 97% and 92% respectively, reaching a clinical concordance of 95%. In comparison, the manual technique showed a greater overlap between the normal and abnormal groups and attained a lower clinical concordance of 85% (data not shown).

The results for the SUSI volumes can be obtained by multiplying the SBR data for the striatum volume of 11.2 ml. The mean (±σ) for normal and abnormal SUSI volumes was 65 (±17) ml and 28 (±13) ml respectively, and the cutoff value between normality and abnormality was 56 ml.

Discussion

A technique has been described for quantification of [^{123}I] FP-CIT images which can provide an accurate measure of the SBR of the tracer, as the ratio between the specific count concentration in the striatum and the non-specific count concentration throughout the brain.

Any SPECT quantitative index is affected by attenuation, scatter/septal penetration and partial volume effects. In this study the loss of counts due to attenuation has been corrected using a simple approximate technique. Use of a more accurate method may result in reduced errors and this will be the subject of further study. No attempt has been made to correct for scatter and septal penetration. This correction, however, can be performed on the acquired projections [23–25] prior to reconstruction of the transaxial images, and therefore is remote from the quantification methodology itself.

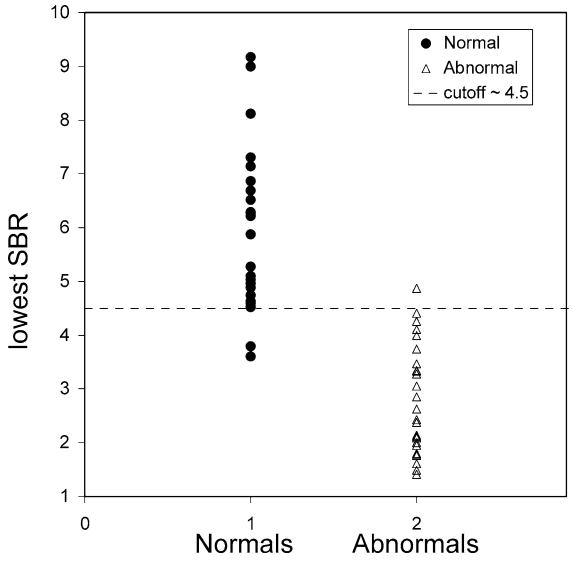

Fig. 6. Minimum SBR between left and right striatum for the two groups of subjects diagnosed as normal (*filled circles*) and abnormal (*open triangles*)

The proposed technique deals with the partial volume effect by measuring the total striatal uptake rather than its concentration. Partial volume effect has a direct impact on measurements of counts concentration, generally leading to an underestimation of the true values. This underestimation depends on the size of the object as well as on the degree of smoothing during reconstruction of the images, and it can be quite considerable for small objects. If the loss of partial volume counts is not accounted for, the measured value for the SBRs will not be a true ratio but rather an index, whose validity is limited to the particular image processing and quantification technique. Furthermore, this correction may be particularly relevant on the basis that the images of PD patients may show greatly reduced functional striatum even at the first presentation of symptoms (which results in very low SBRs, Fig. 6). This appearance reflects the considerable loss of the dopamine transporter mechanism in the very early stages of the disease process [26].

Although the definition of the SBR is commonly based on Eq. 1, the strategies that have been developed to measure it can be quite different, in the choices of the image for the analysis, of the reference region, of the shape and size of the striatal ROIs as well as of the procedure followed for their placement. The majority of the previous studies have determined SBR from measurements of the count concentrations in the striatal VOIs (specific and non-specific) and in the reference region. Their ratio minus 1 is assumed to give SBR as per Eq. 1. The strategy commonly adopted to deal with the partial volume has been to include in the summed image only a subset of the striatal images, that is the central ones with highest signal that are bound to be less affected by partial volume count losses. The chosen thickness of the slab, however, shows a considerable variability between centres, from 7 mm [27] through 20 mm [9] up to 28 mm [10]. With respect to the striatal ROIs, the preferred choice has been the use of templates of anatomical shape, constructed according to a stereotactic brain atlas [8, 29] or obtained from co-registered MRI studies [10], which are manually or automatically [28] placed over the structure. Again, their area shows variability between centres, and sometimes has been kept smaller than the actual structure they represent, to minimise the problem associated with ill definition of the edges due to the poor image resolution [11]. As partial volume correction is not applied, the measured concentrations become dependent on the slab thickness and on the size of the ROIs: the larger the VOI size, the lower the count concentration and the SBR values [29, 30]. More accurate quantitative results could be obtained with the use of 3D iterative algorithms, which incorporate the corrections for attenuation and distance-dependent point spread function in the transition matrix and which can be combined with scatter correction strategies [31]. However, at present their implementation is not widespread.

The method proposed in this paper measures the total striatal counts. The specific count concentration c_s is derived as per Eqs. 4 and 6, and the SBR obtained as per Eq. 7. The dependence of the SBR on the VOI size is thus eliminated (providing that it is sufficiently large to include all partial volume counts) [18]. Again, c_s will not be the "true" value, as the individual volume of the striatum V_s is unknown and a fixed parameter is used in its place. However, V_s appears in Eq. 7 for the SBR as a multiplying factor, and therefore will have no effect on inter-centre variability. The alternative specific uptake size index SUSI (Eq. 5) does express more exactly what is being measured in this technique. The principle of resolution independence of this parameter has been demonstrated with simulation studies [18]. However, it is considered preferable to convert SUSI to an SBR, as this is a more accepted and readily understood concept.

As to the reference region, a variety of brain regions devoid of DATs have been chosen in the literature, such as the cerebellum [32, 33] when imaging with [^{123}I]β-CIT, the occipital cortex [5, 8–10, 28, 34] and the white matter [27] with [^{123}I]β-CIT and [^{123}I]FP-CIT, the frontal cortex [29, 35, 36] with [^{123}I]IBF, [^{123}I]IPT and [^{123}I]FP-CIT, and the supratentorial brain [11, 12, 15, 30] with ^{99m}Tc-TRODAT and [^{123}I]IPT. The general approach is to use standardised templates defined on a brain atlas. Their placement depends on identification of anatomical regions, sometimes aided by the use of the atlas [24, 30, 36] or MR images [10], and therefore is susceptible to operator-introduced variability.

The approach proposed in this paper is to derive the non-specific binding from a region covering the whole cortex in the summed image with the exception of the striatal region. As described, the procedure for the creation of the reference ROI has been fully automated and relies on a 50% iso-contour based on the non-striatum maximum uptake. This automated procedure gives a consistent ROI size in both normal and abnormal scans. Use of the maximum of non-striatal uptake (rather than the maximum in the whole image), in particular, guarantees that the iso-contour is entirely determined by the background distribu-

tion, removing any possible dependence on the relative striatal/background intensity. The exclusion of the peripheral cortex, where the partial volume effect is particularly significant, adds further robustness to the technique.

The issues of variability and reproducibility of DAT quantitative measurements are clearly of importance, particularly in serial investigations. Previous studies have shown that both reproducibility and operator-introduced variability can be improved by increasing the thickness of the summed image [30, 37]. In the interest of reducing observer variability, the use of geometrical ROIs is also advantageous. The anatomical template cannot account for the natural variability in the shape and volume of the corpus striatum, and consequently its placement will require a subjective compromise (unless registration is carried out). A geometrical ROI, on the other hand, can be positioned with a smaller degree of variability.

The comparison with a manual technique that also used geometrical ROIs [16] has allowed the impact on reproducibility of subjective factors other than striatal ROI placement to be assessed. The method proposed in this paper, by eliminating any ambiguity in the extent of the striatal slab and subjectivity in the positioning of the reference ROI, has been shown to decrease the inter-operator COV from 10.6% to a significantly lower value of 3–4%. The smallest change that can be observed with 95% confidence—given by $1.96\sqrt{2}\times$COV—will therefore be 8% for the same operator and 11% for a different operator. It is interesting to note that this is of the same order as the test–retest reproducibility of [^{123}I]FP-CIT studies on normal controls and PD patients, which has been reported to be 8–11% [28, 36].

The current algorithms used for reconstructing the SPECT images do not deal with the influence of counts due to gamma rays scattered in the patient or penetrating through the septa of the collimator. Both these factors reduce the contrast in the images, thus lowering the values of the quantitative indices, such as the SBR, from the truth. Their contribution to the image depends on the detector/collimator combination used during the acquisition, and therefore will limit the validity of the SBR measurements to a particular SPECT system [38]. In order to derive a "universal" index, whose validity is not limited to a particular centre, scatter and septal penetration correction needs to be performed on the acquired projections prior to reconstruction. Once corrected images are inputted, the proposed quantification method should provide an absolute ratio of the striatal specific to non-specific binding that is transferable between centres. Furthermore, the application of this method to a cohort of true controls, rather than to patients with excluded parkinsonism after the [^{123}I]FP-CIT investigation, should permit the identification of a universal cutoff for PS and DLB syndromes.

Finally, the technique is open to further refinements such as the automated positioning of the striatal ROIs and their subdivision into striatal subregions, such as the head of caudate and the putamen tail. Intra-striatal quantification might improve discrimination between normality and disease, as well as yield further information related to disease severity and/or normal aging, particularly relevant in longitudinal studies.

Conclusion

The proposed method for DAT quantification provides an accurate index that correlates well with the clinical findings. The technique is highly reproducible, with an operator-introduced variability of the order of 4%. A cutoff ~4.5 has been identified for the SBR ratio, which separates the diagnosed normal and abnormal groups with a diagnostic concordance of 95%. The cutoff value, however, is currently based on images corrected for attenuation but not for scatter and septal penetration. It is hoped that, once both corrections are incorporated into image processing, the proposed method could provide an accurate cutoff for PS and DLB, universally valid across different cameras.

Acknowledgement. We would like to thank Anne Dawson for her contribution to the assessment of inter-operator variability.

References

1. Brucke T, Asenbaum S, Pirker W, Djamshidian S, Wenger S, Wober C, et al. Measurement of the dopaminergic degeneration in Parkinson's disease with [^{123}I-β-CIT and SPECT. Correlation with clinical findings and comparison with multiple system atrophy and progressive supranuclear palsy. J Neural Transm Suppl 1997;50:9–24
2. Asenbaum S, Pirker W, Angelberger P, Bencsits G, Pruckmayer M, Bruck T. [^{123}I]beta-CIT and SPECT in essential tremor and Parkinson's disease. J Neural Transm 1998;105:1213–1228
3. Benamer TS, Patterson J, Grosset DG, Booij J, de Bruin K, van Royen E, et al. Accurate differentiation of parkinsonism and essential tremor using visual assessment of [^{123}I]-FP-CIT SPECT imaging: the [^{123}I]-FP-CIT study group. Mov Disord 2000;15:503–510
4. Ransmayr G, Seppi K, Donnemiller E, Luginger E, Marksteiner J, Riccabona G, et al. Striatal dopamine transporter function in dementia with Lewy bodies and Parkinson's disease. Eur J Nucl Med 2001;28:1523–1528
5. Walker Z, Costa DC, Walker RWH, Shaw K, Gacinovic S, Stevens T, et al. CLE differentiation of dementia with lewy bodies from Alzheimer's disease using a dopaminergic presynaptic ligand. J Neurol Neurosurg Psychiatry 2002;73:130–140
6. O'Brien JT, Colloby S, Fenwick J, Williams ED, Firbank M, Burn D, et al. Dopamine transporter loss visualised with FP-CIT SPECT in the differential diagnosis of dementia with Lewy bodies. Arch Neurol 2004;61:919–925
7. Marek KL, Seibyl JP, Zoghbi SS, Zea-Ponce Y, Baldwin RM, Fussell B, et al. [^{123}I]beta-CIT/SPECT imaging demonstrates bilateral loss of dopamine transporters in hemi-Parkinson's disease. Neurology 1996;46:231–237
8. Booij J, Tissingh G, Boer GJ, Speelman JD, Stoof JC, Janssen AGM, et al. [^{123}I]FP-CIT SPECT shows a pronounced decline of striatal dopamine transporter labelling in early and advanced Parkinson's disease. J Neurol Neurosurg Psychiatry 1997;62:133–140

9. Booij J, Tissingh G, Winogrodzka A, Boer GJ, Stoof JC, Wolters EC, et al. Practical benefit of [^{123}I]FP-CIT SPECT in the demonstration of the dopaminergic deficit in Parkinson's disease. Eur J Nucl Med 1997;24:68–71
10. Seibyl JP, Marek K, Sheff K, Zoghbi S, Baldwin RB, Charney DS, et al. Iodine-123-β-CIT and iodine-123-FPCIT SPECT measurement of dopamine transporter in healthy subjects and Parkinson's patients. J Nucl Med 1998;39:1500–1508
11. Mozley PD, Scheneider JS, Acton PD, Plössl K, Stern MB, Siderowf A, et al. Binding of [^{99m}Tc]TRODAT-1 to dopamine transporters in patients with Parkinson's disease and in healthy volunteers. J Nucl Med 2000;41:584–589
12. Tatsch K, Schwarz J, Mozley PD, Linke R, Pogarell O, Oertel WH, et al. Relationship between clinical features of Parkinson's disease and presynaptic dopamine transporter binding assessed with [^{123}I]IPT and single-photon emission tomography. Eur J Nucl Med 1997;24:415–421
13. Laruelle M, Wallace E, Seibyl JP, Baldwin RM, Zea-Ponce Y, Zoghbi SS, et al. Graphical, kinetic and equilibrium analyses of in vivo [^{123}I]β-CIT binding to dopamine transporter in healthy human subjects. J Cereb Blood Flow Metab 1994;14:982–994
14. Booij J, Hemelaar JTGM, Speelman JD, de Bruin K, Janssen GM, van Royen EA. One-day protocol for imaging of the nigrostriatal dopaminergic pathway in Parkinson's disease by [^{123}I]FPCIT SPECT. J Nucl Med 1999;40:753–761
15. Acton PD, Meyer PT, Mozley PD, Plössl K, Kung HF. Simplified quantification of dopamine transporters in humans using [^{99m}Tc]TRODAT-1 and single-photon emission tomography. Eur J Nucl Med 2000;27:1714–1718
16. Costa DC, Walker Z, Dizdarevic S, Ioannides C, Gacinovic S, Walker RW, et al. Striatal binding index of FP-CIT: a simple method to separate Parkinson's disease patients and controls [abstract]. Eur J Nucl Med 1998;25:1069
17. Bolt L, Fleming JS, Hoffmann SMA, Kemp PM, Costa DC. Quantifying DaTSCAN images: how automation reduces operator variability. Nucl Med Commun 2003;24:445
18. Fleming JS, Bolt L, Stratford JS, Kemp PM. The specific uptake size index for quantifying radiopharmaceutical uptake. Phys Med Biol 2004;49:N227–N234
19. Blinkov SM, Glezer II. The human brain in figures and tables. A quantitative handbook. New York: Basic Books, Plenum Press; 1968. pp 166–171
20. Aylward EH, Li Q, Habbak R, Warren A, Pulsifer MB, Barta PE, et al. Basal ganglia volume in adults with Down syndrome. Psychiatry Res Neuroimaging Section 1997;74: 73–82
21. JL Fleiss. Statistical methods for rates and proportions. 2nd ed. New York: Wiley; 1981
22. Bland JM, Altman DG. Statistical method for assessing agreement between two methods of clinical measurement. Lancet 1986;1:307–310
23. Fleming JS, Alaamer AS. Influence of collimator characteristics on quantification in SPECT. J Nucl Med 1996;37:1832–1836
24. Hashimoto J, Sasaki T, Ogawa K, Kubo A, Motomura N, Ichihara T, et al. Effects of scatter and attenuation correction on quantitative analysis of β-CIT brain SPECT. Nucl Med Commun 1999;20:159–165
25. Kim KM, Varrone A, Watabe H, Shidahara M, Fujita M, Innis RB, et al. Contribution of scatter and attenuation compensation to SPECT images of nonuniformly distributed brain activities. J Nucl Med 2003;44:512–519
26. Parkinson Study Group. Dopamine transporter brain imaging to assess the effect of pramipexole vs levadopa on Parkinson disease progression. JAMA 2002;13:1653–1661
27. Kuikka JT, Bergstrom KA, Ahonen A, Hiltunen J, Haukka J, Länsimies E, et al. Comparison of iodine-123 labelled 2β-carbomethoxy-3β-(4-iodophenyl)tropane and 2β-carbometho xy-3β-(4-iodophenyl)-*N*-(3-fluoropropyl)nortropane for imaging the dopamine transporter in the living human brain. Eur J Nucl Med 1995;22:356–360
28. Booij J, Habraken JBA, Bergmans P, Tissingh G, Winogrodzka A, Wolters EC, et al. Imaging of dopamine transporter with iodine-123-FP-CIT SPECT in healthy controls and patients with Parkinson's disease. J Nucl Med 1998;39:1879–1884
29. Ichise M, Ballinger JR, Tanaka F, Moscovitch M, St. George-Hyslop PH, Raphael D, et al. Age-related changes in D_2 receptor binding with iodine-123-iodobenzofuran SPECT. J Nucl Med 1998;39:1511–1518
30. Linke R, Gostomzyk J, Hahn K, Tatsch K. [^{123}I]IPT binding to presynaptic dopamine transporter: variation of intra- and interobserver data evaluation in parkinsonian patients and controls. Eur J Nucl Med 2000;27:1809–1812
31. Cot A, Falcón C, Crespo C, Sempau J, Pareto D, Bullich S, et al. Absolute quantification of dopaminergic neurotransmission SPECT using a Monte Carlo-based scatter correction and fully 3-dimensional reconstruction. J Nucl Med 2005;46: 1497–1504
32. Pirker W, Asenbaum S, Bencsits G, Prayer D, Gerschlager W, Deecke L, et al. [^{123}I]-β-CIT SPECT in multiple system atrophy, progressive supranuclear palsy, and corticobasal degeneration. Mov Disord 2000;15:1158–1167
33. Pirker W, Asenbaum S, Hauk M, Kandlhofer S, Tauscher J, Willeit M, et al. Imaging serotonin and dopamine transporters with^{123}I-beta-CIT SPECT: binding kinetics and effects of normal aging. J Nucl Med 2000;41:36–44
34. van Dyck CH, Seibyl JP, Malison RT, Laurelle M, Wallace E, Zoghbi SS, et al. Age-related decline in striatal dopamine transporter binding with iodine-123-β-CIT SPECT. J Nucl Med 1995;36:1175–1181
35. Schwarz J, Storch A, Koch W, Pogarelli O, Radau PE, Tatsch K. Loss of dopamine transporter binding follows a single exponential rather than linear decline. J Nucl Med 2004;45:1694–1697
36. Tsuchida T, Ballinger JR, Vines D, Kim YJ, Utsunomiya K, Lang AE, et al. Reproducibility of dopamine transporter density measured with ^{123}I-FPCIT SPECT in normal control and Parkinson's disease patients. Ann Nucl Med 2004;18:609–616
37. Seibyl JP, Laurelle M, van Dick CH, Wallace E, Baldwin RM, Zoghbi S, et al. Reproducibility of iodine-123-β-CIT SPECT brain measurement of dopamine transporters. J Nucl Med 1996;37:222–228
38. Meyer PT, Sattler B, Lincke T, Seese A, Sabri O. Investigating dopaminergic neurotransmission with ^{123}I-FP-CIT SPECT: comparability of modern SPECT systems. J Nucl Med 2003; 45:839–845